Pentalenene Synthase. Purification, Molecular Cloning, Sequencing, and High-Level Expression in Escherichia coli of a Terpenoid Cyclase from Streptomyces UC5319

ARTICLE *in* BIOCHEMISTRY · JUNE 1994

Impact Factor: 3.02 · DOI: 10.1021/bi00185a024 · Source: PubMed

8 AUTHORS, INCLUDING:

Jae Kyung Sohng
Sun Moon University
279 PUBLICATIONS **2,224** CITATIONS
SEE PROFILE

Suzanne M. Rudnicki
Brown University
3 PUBLICATIONS **132** CITATIONS
SEE PROFILE

John Oliver
Nabsys, Inc.
25 PUBLICATIONS **1,386** CITATIONS
SEE PROFILE

Journal of
Nanoscience and Nanotechnology
Vol. 12, 1–12, 2012

Antibacterial Activity and Increased Freeze-Drying Stability of Sialyllactose-Reduced Silver Nanoparticles Using Sucrose and Trehalose

Hwa Jung Noh[1], A-Rang Im[2], Hyun-Seok Kim[3], Jae Kyung Sohng[4], Chong-Kook Kim[1], Yeong Shik Kim[2], Seonho Cho[3,*], and Youmie Park[1,3,*]

[1] *College of Pharmacy, Inje University, 607 Obang-dong, Gimhae, Gyeongnam 621-749, Republic of Korea*
[2] *Natural Products Research Institute, College of Pharmacy, Seoul National University, 599 Gwanangno, Gwanak-gu, Seoul 151-742, Republic of Korea*
[3] *National Creative Research Initiatives (NCRI) Center for Isogeometric Optimal Design, Seoul National University, 599 Gwanangno, Gwanak-gu, Seoul 151-744, Republic of Korea*
[4] *Institute of Biomolecule Reconstruction, Department of Pharmaceutical Engineering, Sun Moon University, 100 Kalsan-ri, Tangjeongmyun, Asansi, Chungnam 336-708, Republic of Korea*

The resistance to current antibiotics results in the emergence of health-threatening bacteria. Silver nanoparticles are known to exhibit broad-spectrum antibacterial activities without the development of resistance. Herein, we developed a green synthetic method for the preparation of silver nanoparticles with sialyllactose instead of toxic chemicals as a reducing agent, which would improve its therapeutic applicability and increases its biocompatibility. Oven incubation, autoclaving and microwave irradiation methods were applied to prepare the silver nanoparticles. High resolution-transmission electron microscopy and atomic force microscopy images revealed mostly spherical and amorphous silver nanoparticles with an average diameter of 23.64 nm. Fourier Transform-infrared spectra suggest that the N–H amide of sialyllactose might be involved in the binding of silver nanoparticles. Based on thermogravimetric analyses, 2,3-sialyllactose-reduced silver nanoparticles are composed of 54.3 wt% organic components and 45.7 wt% metallic silver. Enhanced antibacterial activities of silver nanoparticles of approximately 8-fold were observed against *Pseudomonas aeruginosa*, *Escherichia coli* and *Salmonella typhimurium* (minimum inhibitory concentration 16 μg/mL). Next, we employed the use of carbohydrate stabilizers to increase the stability of silver nanoparticles during a freeze-drying process. It was found that sucrose and trehalose were the most effective stabilizers. In addition, silver nanoparticles possessed excellent salt stability as well as on-the-shelf stability in the presence of these stabilizers. Derivatives of sialic acid are known to be anti-influenza agents; therefore, the newly prepared silver nanoparticles may serve as useful antibacterial and antiviral agents to cope with both pathogenic bacteria and viruses in the near future.

Keywords: Silver Nanoparticles, Sialyllactose, Antibacterial Activity, Freeze-Drying, Sucrose, Trehalose.

RESEARCH ARTICLE

1. INTRODUCTION

Multidisciplinary research in nanotechnology, biology and medicine has given rise to mimetics of natural molecules in the nanoscale range. Among the mimetics, metallic nanoparticles have received great attention due to their potential applications. Silver (Ag) has been used for centuries in the treatment of bacterial infections, especially wound infections in burn patients, as well as for hygiene, personal care and healthcare.[1] The development of novel Ag nanomaterials have been found to be applicable to diverse medical applications such as Ag-coated medical devices and Ag dressings.[2,3] Due to the frequent occurrence of multi-drug resistance to antibiotics, silver nanoparticles (AgNPs) have emerged as potential inorganic antibacterial agents with a broad spectrum. AgNPs possess antibacterial activity against a variety of drug-resistant pathogenic bacteria such as methicillin-resistant *Staphylococcus aureus* (MRSA), ampicillin-resistant *Escherichia coli* O157:H7, erythromycin-resistant *Streptococcus pyogenes* and multidrug-resistant *Pseudomonas aeruginosa*.[4,5]

*Authors to whom correspondence should be addressed.

In addition, AgNPs exhibit synergistic effects with antibiotics against gram-positive and gram-negative bacteria.[6] Ag acts as an antibacterial agent by binding structural proteins and DNA bases.[7] Additional effects of AgNPs were observed when the topical delivery of AgNPs promoted wound healing in an animal model.[8] Recently, AgNPs have been reported as potential antiviral agents against the human immunodeficiency, hepatitis B, herpes simplex, respiratory syncytial, tacaribe and monkey pox viruses.[9]

AgNPs are commonly synthesized using chemical reducing agents. Currently, the "green synthesis" of metallic nanoparticles has emerged as an environmentally benign process. In the green synthesis of AgNPs, the use of biological entities instead of toxic chemicals has been reviewed.[10, 11] Wei et al. reported the "green synthesis" of AgNPs by reducing Ag salts with nontoxic and biodegradable chitosan.[12] The chitosan-reduced AgNPs exhibited highly potent antibacterial activity toward both Gram-positive and Gram-negative bacteria. Sialic acids play important roles in biological, immunological and pathological processes.[13] Sialyllactose-carrying clusters such as dendrimers and polystyrenes have been reported to be inhibitors of influenza viruses.[14–16] A trivalent anti-influenza reagent was developed in which sialyllactose was located at the end of each valence.[17] Johansson et al. reported a synthetic route for human serum albumin conjugates carrying 2,3-sialic acid that effectively prevent adenovirus from binding and infecting to the host cells.[18] Sialic acid-terminated glycerol dendron functionalized onto gold nanoparticles showed inhibitory activity against the influenza virus by preventing plasma membrane binding.[19]

In the present research, we used 2,3- and 2,6-sialyllactose as reducing agents in the green synthesis of AgNPs. The formation of AgNPs was confirmed by surface plasmon resonance (SPR), high resolution-transmission electron microscopy (HR-TEM), atomic force microscopy (AFM), Fourier-Transform infrared (FT-IR) and differential thermal analysis/thermogravimetric analysis (DTA/TGA). Three different methods of synthesis (oven incubation, autoclaving and microwave irradiation) were tested. We also assessed the impact of stabilizers on AgNPs stability during a freeze-drying process. The salt and on-the-shelf stabilities were tested before and after the addition of stabilizers. The antibacterial activity of newly prepared AgNPs was tested against a total of twenty Gram-positive and Gram-negative bacteria strains to ensure their applicability in pharmaceutical and biomedical applications.

2. MATERIALS AND METHODS

2.1. Chemicals and Instruments

Dextran (266 kDa), mannitol, sucrose, trehalose and $AgNO_3$ were purchased from Sigma-Aldrich (St. Louis, MO, USA). All other reagents were of analytical grade. Double-distilled water was used. 2,3- and 2,6-Sialyllactose were from GenChem (Daejeon, Korea, the structures in Fig. 1). UV-Vis spectra of the nanoparticles were measured using a Jasco V-550 UV spectrophotometer with a quartz cuvette (JEOL Ltd., Tokyo, Japan). HR-TEM was performed to obtain images of the nanoparticles on a JEM-3010 model operating at 300 kV (JEOL Ltd., Tokyo, Japan). Before HR-TEM imaging, the AgNPs solution was placed on a carbon grid (carbon type-B, 300 mesh, Ted Pella Inc., Redding, CA, USA) and dried overnight in a 37 °C oven. The freeze-drying process was performed on a FD5505 model freeze-dryer with a vacuum condition of 5 mTorr with the temperature maintained at −50 °C (IlShinBio, Seoul, Korea). FT-IR spectra were recorded on a FT-IR 4200 with a KBr pellet method (JASCO Co, Tokyo, Japan). For DTA/TGA analyses, the freeze-dried samples were placed in platinum sample pans and heated under a nitrogen atmosphere from 20 °C to 400 °C at a rate of 10 °C/min by a simultaneous DTA/TGA analyzer Q600 (TA Instruments, New Castle, USA). The autoclave (model ST01060) was purchased from Daihan Scientific (Seoul, Korea). Microwave irradiation was performed with a microwave oven (model MR280M; LG Electronics, Seoul, Korea). AFM images were obtained using a Dimension® Icon® (Bruker Nano, Inc., Santa Barbara, CA, USA) with a tapping mode using a RTESP probe (MPP-11100-10, premium high-resolution tapping mode silicon probe, Bruker Nano, Inc., Santa Barbara,

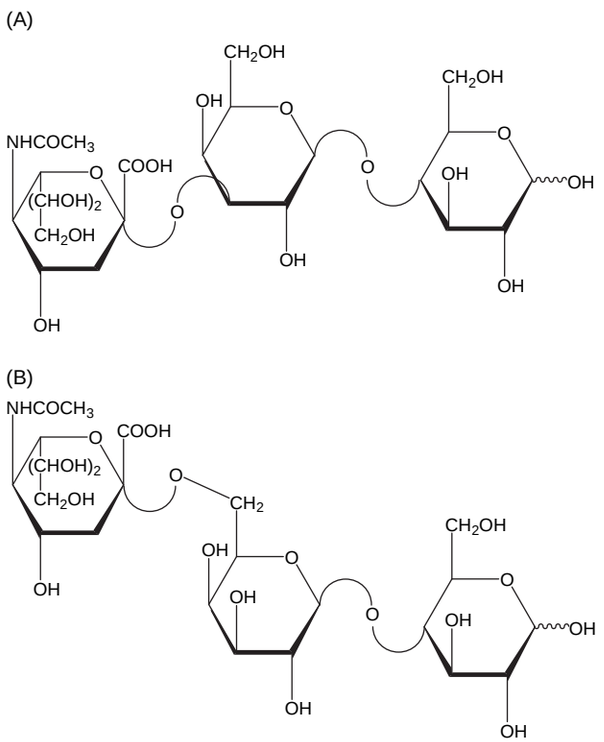

Fig. 1. The structure of (A) 2,3-sialyllactose and (B) 2,6-sialyllactose used in this study.

California, USA). The sample solutions were placed onto a freshly cleaved mica (grade V-1, 25 mm by 25 mm length, 0.15 mm thick, SPI Supplies Division of Structure Probe, Inc., West Chester, PA, USA) and were dried in a 37 °C oven for 6 h prior to analysis.

2.2. Green-Synthesis of Sialyllactose-Reduced AgNPs

To optimize the reaction conditions for the synthesis of AgNPs, the $AgNO_3$ concentration (0.05–5 mM), 2,3- and 2,6-sialyllactose concentration (0.1–10 mM) and reaction times (0–21 h) were varied. The optimized reaction conditions were tested by oven incubation at 95 °C. One condition was varied while the others were fixed. For the synthesis of AgNPs, a preincubation step was performed; an aqueous solution of 500 μL of $AgNO_3$ (0.5 mM) was heated and stirred until boiling. A solution of 500 μL of 2,3- or 2,6-sialyllactose (1.0 mM) was added dropwise to the $AgNO_3$ solution and heated to boiling.[20] The solution turned from colorless to light yellow, indicating the initial formation of AgNPs (preincubation step). Next, the solution was placed in an oven at 95 °C (oven incubation method). The formation of AgNPs was confirmed by UV-Vis spectra with a characteristic SPR band at 422–424 nm. Upon optimization of the reaction conditions with the oven method, the same composition of $AgNO_3$ and sialyllactose was used for autoclaving and microwave irradiation. For the autoclaving method, the optimized composition of $AgNO_3$ and sialyllactose was autoclaved at 15 psi, 125 °C for 15 min. The microwave irradiation method used a microwave oven at a power of 700 W for 10 min.

2.3. Antibacterial Activity of Sialyllactose-Reduced AgNPs

The sialyllactose-reduced AgNPs prepared by autoclaving were used for antibacterial activity tests. The antibacterial activities were determined by the minimal inhibitory concentration (MIC). The measurement of MIC values were conducted in accordance with the recommendations of the Clinical Laboratory Standards Institute (CLSI: formerly the National Committee for Clinical Laboratory Standards)[21] where Muller Hilton agar plates containing 5% sheep blood was used. For the subculture of *Streptococcus pyogenes*, Muller Hilton II agar plates with 5% lysed horse blood was used while Muller Hilton I agar plates were used for the subculture of the other strains. For comparing purposes, norfloxacin was selected as a standard antibiotic. On Muller Hilton I agar plates, bacterial broth cultures were added and distributed on the plates uniformly. Sterile paper discs were prepared, wetted with samples and placed on the plates. Then, the incubation was performed at 36 °C for 24 h. After incubation, the measurement was conducted on the diameters of the inhibitory zones (mm) around the disks. The minimum inhibitory concentration (MIC μg/mL) was defined by the lowest concentration that inhibited bacterial growth. MIC values were calculated based on sialyllactose concentration.

2.4. Addition of Stabilizers for a Freeze-Drying Process

To select efficient stabilizers during a freeze-drying process, we tested four different carbohydrates on 2,3-sialyllactose-reduced AgNPs; dextran (0.3–1.3%), sucrose (50–250 mM), trehalose (50–250 mM), and mannitol (50–250 mM). Before the freeze-drying process, each stabilizer was added in two different reaction steps for comparison purposes:

(1) each stabilizer was added dropwise while stirring when mixing the solutions of $AgNO_3$ with sialyllactose on the hot plate (preincubation step) or

(2) each stabilizer was added after the formation of AgNPs by the oven method.

The final volume of the AgNPs solution was adjusted to 1.5 mL by the addition of water to make a fixed final

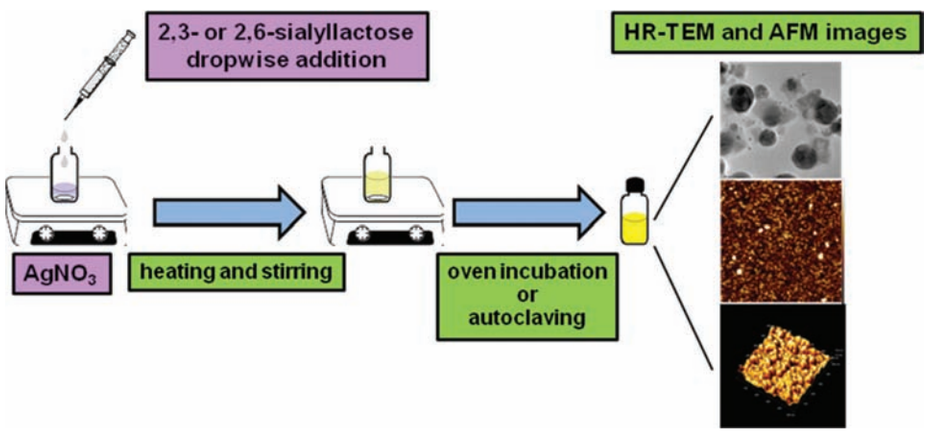

Fig. 2. The schematic representation of AgNPs formation by sialyllactose. The photographs show HR-TEM (top) and AFM (middle and bottom) images of sialyllactose-reduced AgNPs. The images exhibited mostly spherical and amorphous shapes. The average diameter was measured to be 23.64 nm.

RESEARCH ARTICLE

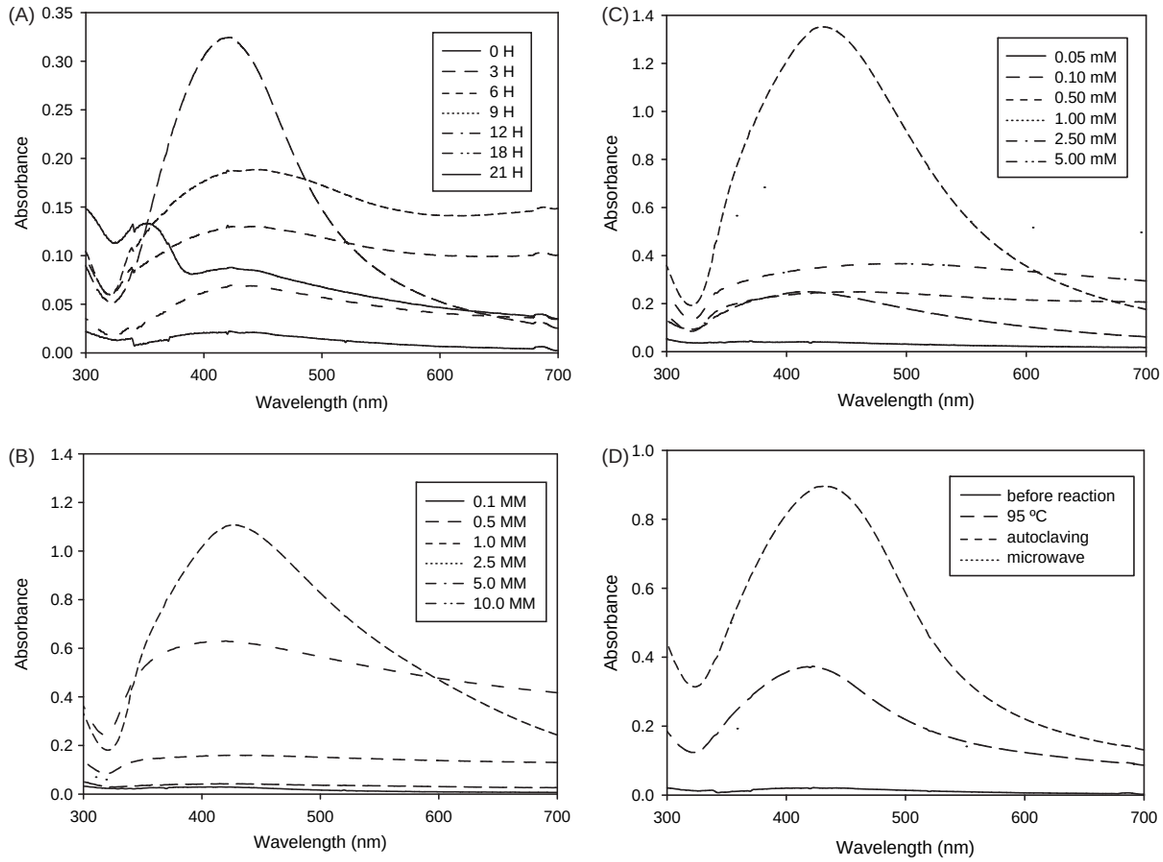

Fig. 3. SPR bands during reaction optimization of 2,3-sialyllactose-reduced AgNPs. (A) changes in reaction time (0–21 h), (B) changes in 2,3-sialyllactose concentration (0.1–10 mM), (C) changes in $AgNO_3$ concentration (0.05–5 mM), and (D) a comparison of three different methods—oven incubation at 95 °C, autoclaving and microwave irradiation.

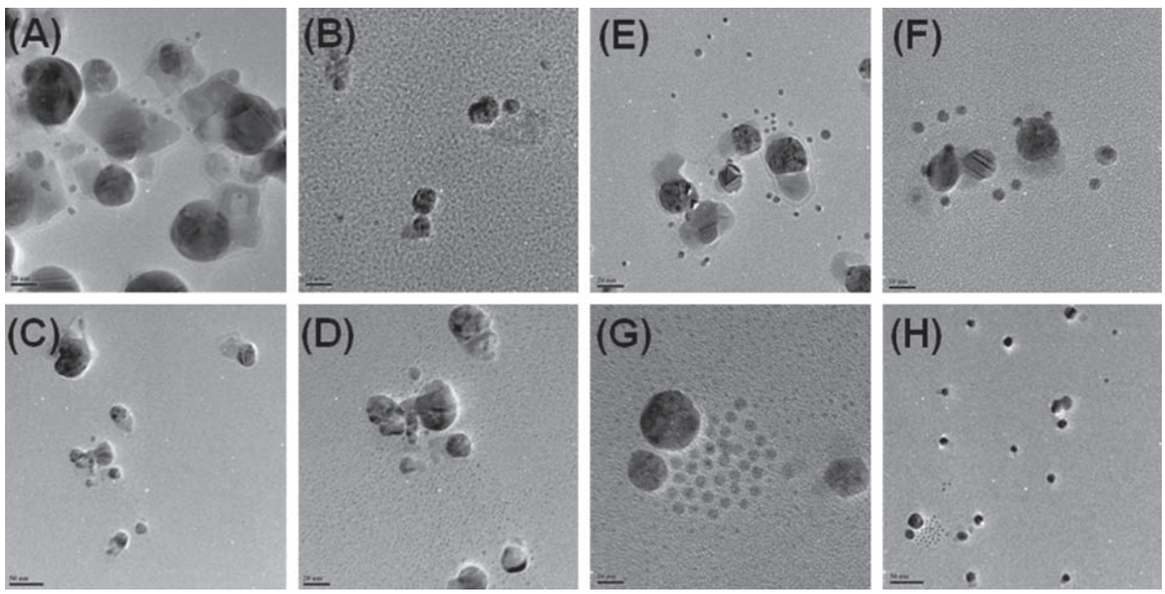

Fig. 4. HR-TEM images of 2,3-sialyllactose-reduced AgNPs. (A) (B) 95 °C oven incubation was performed, and (C) (D) an autoclaving method was employed. The scale bar represents (A) 20 nm, (B) 20 nm, (C) 50 nm, and (D) 20 nm. HR-TEM images of 2,6-sialyllactose-reduced AgNPs. (E) (F) 95 °C oven incubation was performed, and (G) (H) an autoclaving method was employed. The scale bar represents (E) 20 nm, (F) 10 nm, (G) 10 nm, and (H) 50 nm, respectively.

RESEARCH ARTICLE

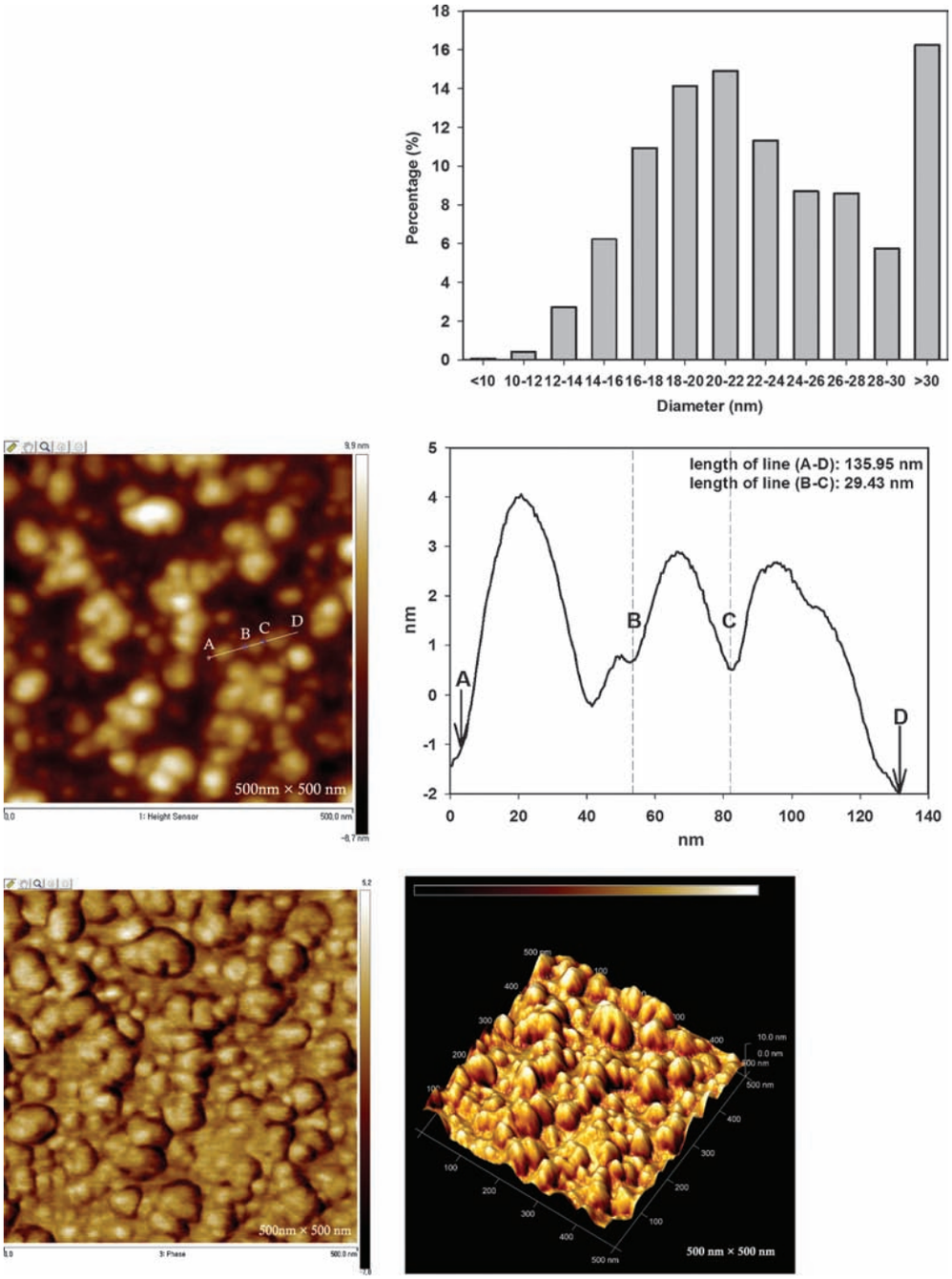

Fig. 5. AFM images of 2,3-sialyllactose-reduced AgNPs. The number of sample points of the X and Y axes are 1024. The scan size of (A) is 2.5 μm by 2.5 μm, and the scan size of (B), (C), and (D) is 500 nm by 500 nm. (A) 3-dimensional height image (A-1) with a diameter histogram (A-2). The histogram was obtained from a total of 3,128 nanoparticles from the image. (B) 2-dimensional height image (B-1) with a section analysis (B-2), (C) 2-dimensional phase image, and (D) 3-dimensional phase image.

volume of each sample for recording UV-Vis absorbance. The sample was placed in a deep-freezer at −80 °C for an hour and then kept in a freeze-dryer for 36 h. After freeze-drying, each sample containing a stabilizer was reconstituted with water to a final volume of 1.5 mL, and UV-Vis spectra were obtained. The morphology, size and dispersion state of AgNPs were confirmed by HR-TEM and AFM images.

2.5. Salt and On-the-Shelf Stabilities

To demonstrate the salt stability of the AgNPs, the 2,3-sialyllactose-reduced AgNPs (900 μL) prepared according

to the optimized reaction conditions were mixed with 100 μL of different concentrations of NaCl solutions (50 mM, 100 mM, 250 mM, 500 mM, 1 M and 2 M). Next, the change of the SPR band was observed by UV-Vis. To investigate the impact of a stabilizer in salt solutions, the AgNP solution containing a stabilizer (50 mM sucrose or 50 mM trehalose) was subjected to the addition of NaCl solutions. Additionally, the AgNPs solution with a stabilizer was freeze-dried and reconstituted with water, and the salt stability was then measured by the method stated above. The on-the-shelf stability was also tested at room temperature. The AgNP solution treated with a stabilizer (50 mM sucrose or 50 mM trehalose) before and after freeze-drying was put on the shelf, and the UV-Vis spectra were recorded at 1-week intervals.

3. RESULTS AND DISCUSSION

3.1. Green Synthesis and Characterization of Sialyllactose-Reduced AgNPs

The schematic representation of AgNPs formation is shown in Figure 2. The SPR of AgNPs is responsible for their yellow color in solution. The color of the solution changes from colorless to yellow after the reaction. Therefore, the formation of AgNPs was monitored visually as well as by recording the UV-Vis absorbance with its characteristic band at 422–424 nm. To optimize the reaction conditions, three factors (sialyllactose concentration, $AgNO_3$ concentration and reaction time) were varied. As shown in Figure 3(A), the optimum reaction time, at which the UV-Vis absorbance was at a maximum, was 3 h. The optimum concentrations of 2,3-sialyllactose and $AgNO_3$ were found to be 1.0 and 0.5 mM, respectively (Figs. 3(B and C)). Among the three different methods tested, the autoclaving method exhibited the highest absorbance, followed by oven incubation and microwave irradiation (Fig. 3(D)). The same reaction optimization results were obtained with 2,6-sialyllactose-reduced AgNPs (data not shown). HR-TEM images exhibited mostly spherical and amorphous shapes in both 2,3- and 2,6-sialyllactose-reduced AgNPs (Fig. 4). The smallest diameter was observed at ~0.3 nm and the largest diameter was found to be ~57 nm. The formation of 2,3-sialyllactose-reduced AgNPs was clearly observed in the AFM images (Figs. 5(A–D)). In a 3-dimensional height image (Fig. 5(A)), the average diameter of AgNPs was measured to be 23.64 nm where a total number of 3,128 nanoparticles in the image were used for a

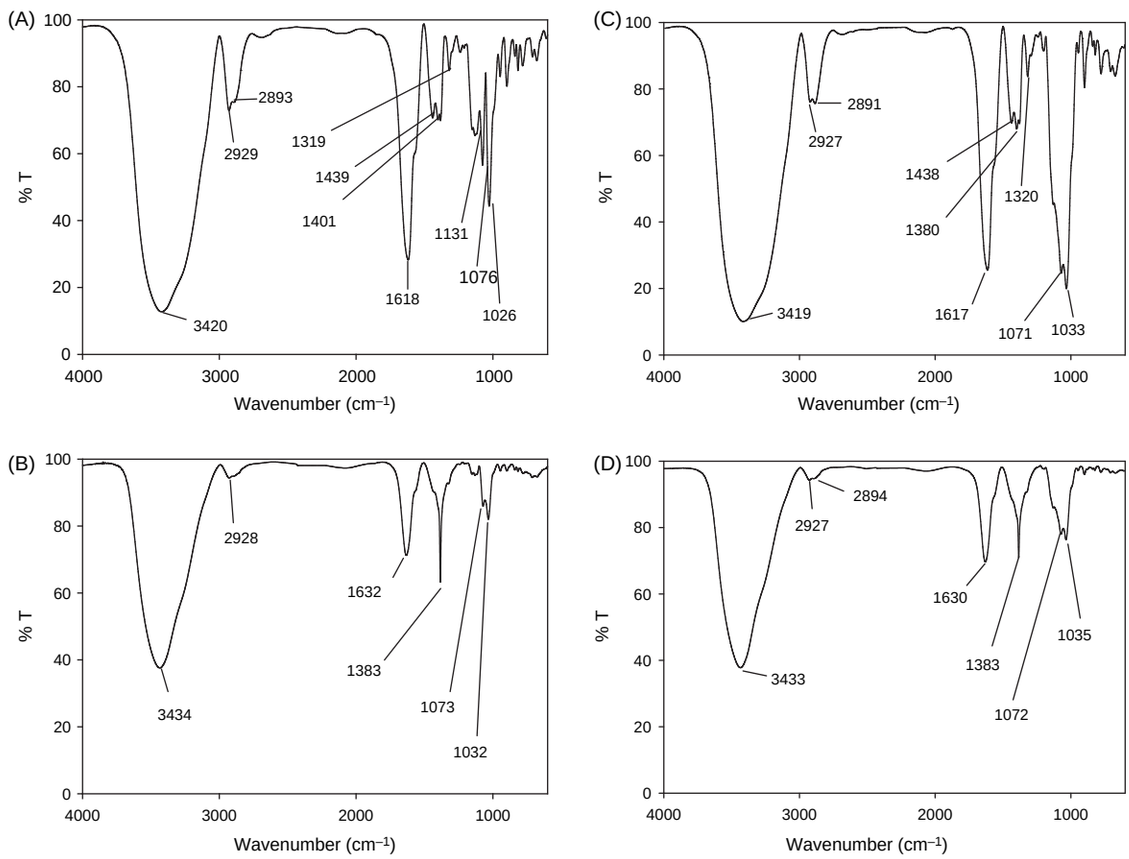

Fig. 6. FT-IR spectra of (A) 2,3-sialyllactose, (B) 2,3-sialyllactose-reduced AgNPs, (C) 2,6-sialyllactose, and (D) 2,6-sialyllactose-reduced AgNPs.

measurement. Up to a diameter of 30 nm, the histogram showed a Gaussian distribution. The AgNPs, which were most abundant had a diameter >30 nm (16.2%), which possibly originated from the agglomeration of nanoparticles having amorphous shapes. The next abundant diameter was 20–22 nm (14.9%) followed by 18–20 nm (14.1%) and 22–24 nm (11.3%). A closer view of the height image is shown in Figure 5(B) with a section analysis. The height of one representative AgNP is ∼2.5 nm and the length between the bars (line B–C in Fig. 5(B)) is 29.43 nm. As previously mentioned in HR-TEM images (Fig. 4), mostly spherical and amorphous shapes of AgNPs were also observed in the 2- and 3-dimensional phase images (Figs. 5(C and D)).

To further confirm the formation of AgNPs with sialyllactose, FT-IR spectra were obtained. Figures 6(A) and (C) show the spectra of 2,3-sialyllactose and 2,6-sialyllactose, respectively. Both spectra show a fingerprint region of the overlap of N–H and O–H stretching vibrations of sialyllactose, which manifests as a strong band at 3300–3500 cm^{-1}. After reducing $AgNO_3$ with sialyllactose, the transmittance of this band was increased, suggesting that absorbance was decreased (Figs. 6(B and D)). The decrease of absorbance in this band region may indicate that the O–H and N–H stretching vibration was influenced by the formation of AgNPs. This result suggests that a nitrogen atom may be involved in the binding of AgNPs, resulting in an absorbance decrease. An increased transmittance of the stretching vibration region of N–H and O–H during the formation of AgNPs has been reported previously.[22] This observation is opposite to that of lead adsorption on chitosan/PVA hydrogel beads, in which the transmittance of the N–H and O–H stretching vibrations of chitosan were decreased,[23] possibly because both N–H and O–H bonds might have different mechanisms when absorbing AgNPs and lead ions. The characteristic amide C═O stretching vibration was observed at 1617–1618 cm^{-1}. This band was also affected, shifting its wavenumber to 1630–1632 cm^{-1}. Other changes were observed at wavenumbers 1439 and 1401 cm^{-1}, which are closely related to

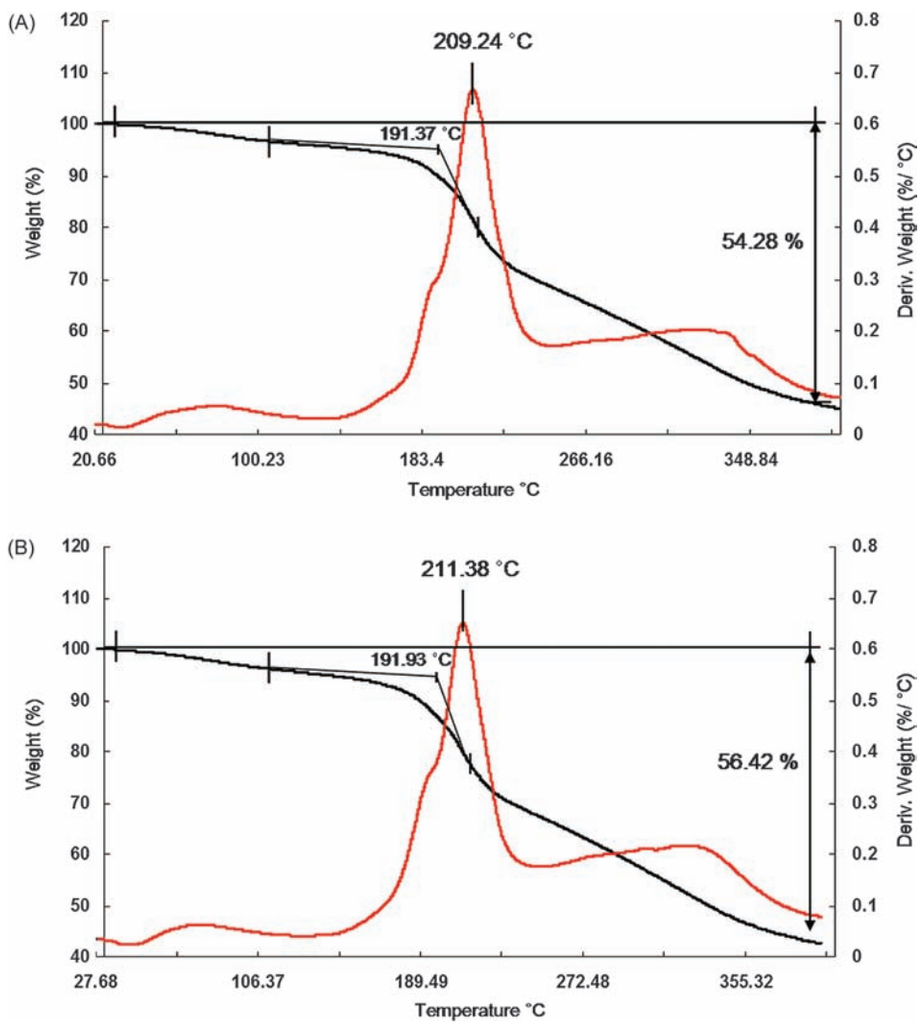

Fig. 7. TGA data of (A) 2,3-sialyllactose-reduced AgNPs and (B) 2,6-sialyllactose-reduced AgNPs.

RESEARCH ARTICLE

Table I. Antibacterial activities of sialyllactose and sialyllactose-reduced AgNPs.

Strain names		MIC (μg/mL)[a]				
		2,3-sialyllacotse-reduced AgNPs	2,3-sialyllactose	2,6-sialyllactose-reduced AgNPs	2,6-sialyllactose	Norfloxacin[b]
Staphylococcus	*aureus* SG511	64	>128	64	>128	≤0.03
Staphylococcus	*aureus* 285	64	>128	64	>128	0.5
Staphylococcus	*aureus* 503	32	>128	64	>128	0.5
Streptococcus	*pyogenes* 308A	>128	>128	>128	>128	4
Streptococcus	*pyogenes* T 12 A	>128	>128	>128	>128	0.13
Streptococcus	*pyogenes* 77 A	>128	>128	>128	>128	0.13
Pseudomonas	*aeruginosa* 9027	16	>128	16	>128	0.5
Pseudomonas	*aeruginosa* 1592E	16	>128	32	>128	0.12
Pseudomonas	*aeruginosa* 1771	32	>128	32	>128	0.6
Pseudomonas	*aeruginosa* 1771M	16	>128	32	>128	≤0.03
Escherichia	*coli* 078	16	>128	16	>128	≤0.03
Escherichia	*coli* TEM	16	>128	16	>128	≤0.03
Escherichia	*coli* 1507	32	>128	32	>128	≤0.03
Escherichia	*coli* DC 0	64	>128	32	>128	0.6
Escherichia	*coli* DC 2	32	>128	16	>128	≤0.03
Salmonella	*typhimurium*	32	>128	16	>128	≤0.03
Klebsiella	*oxytoca* 1082E	32	>128	32	>128	≤0.03
Klebsiella	*areogenes* 1522E	32	>128	32	>128	≤0.03
Enterobacter	*cloacae* P99	32	>128	32	>128	≤0.03
Enterobacter	*cloacae* 1321E	32	>128	32	>128	≤0.03

[a]MIC values were calculated based on sialyllactose concentration. [b]Norfloxacin was used as a standard antibiotic.

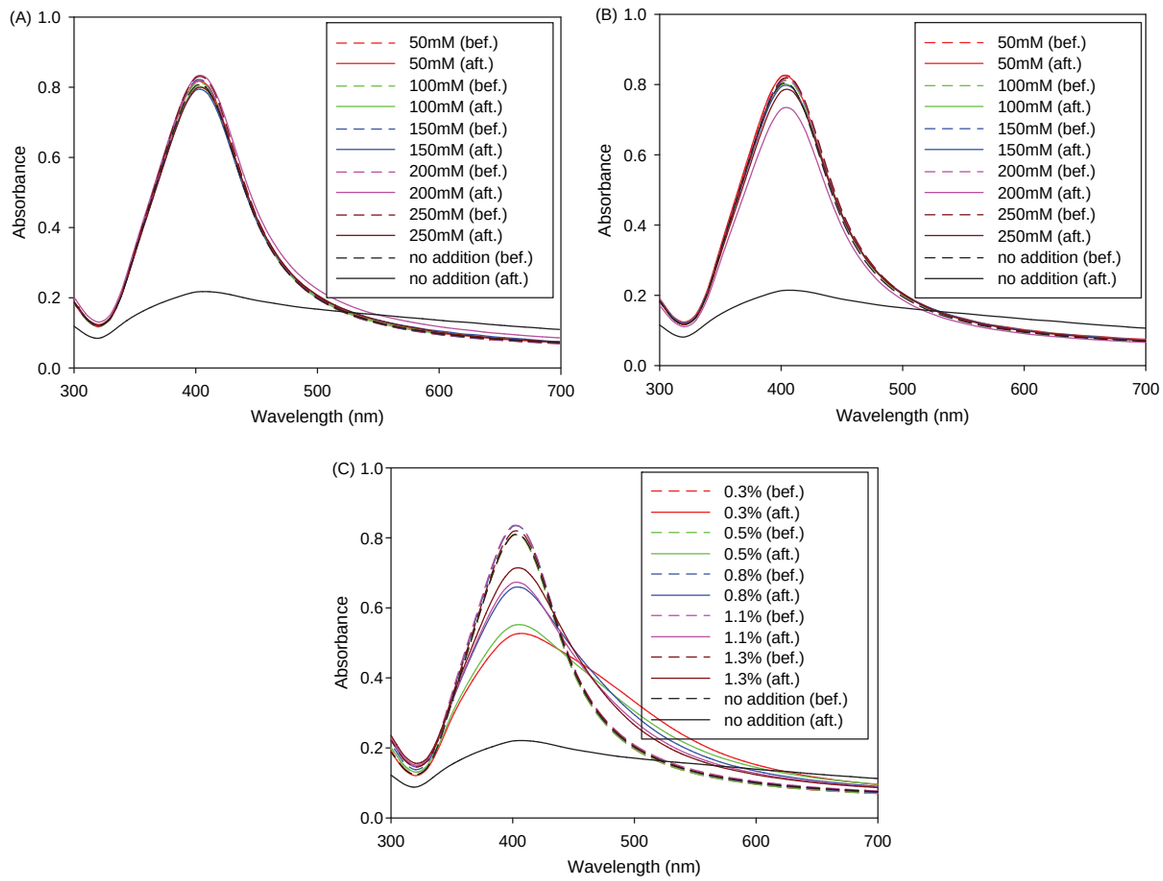

Fig. 8. UV-Vis spectra of AgNPs before and after freeze-drying. Each stabilizer was added after incubation in the oven. (A) sucrose, (B) trehalose, and (C) dextran. The legends in the inset 'bef.' and 'aft.' represent 'before freeze-drying' and 'after freeze-drying'.

N–H amide and CH_2 bending vibrations. These bands were shifted to a lower wavenumber at 1383 cm^{-1}, suggesting the involvement of nitrogen atoms in the binding of AgNPs. AgNPs are not likely to bind to carbon atoms; therefore, it is more likely that AgNPs are bound to the nitrogen atom of sialyllactose, leading to an increase in molecular weight. Thus, the vibration of the N–H amide was reduced to a lower wavenumber. As shown in Figure 7(A), in the DTA/TGA analyses, 2,3-sialyllactose-reduced AgNPs are composed of 54.3 wt% organic components and 45.7 wt% inorganic components, which are mostly metallic silver. Similar results were obtained from 2,6-sialyllactose-reduced AgNPs: 56.4 wt% organic components and 43.6 wt% metallic silver (Fig. 7(B)).

3.2. Antibacterial Activity of Sialyllactose-Reduced AgNPs

The results of the MIC tests are listed in Table I. MIC values were calculated based on sialyllactose concentration. MIC values of sialyllactose exhibited >128 μg/mL of all 20 bacteria strains tested, while sialyllactose-reduced AgNPs displayed antibacterial activities with MIC values ranging from 16 to 128 μg/mL. This result implies that the antibacterial activity of sialyllactose-reduced AgNPs was possibly originated from AgNPs. The antibacterial activity of AgNPs has been reported in many previous literatures.[10, 24–26] Interestingly, MIC values of Gram-negative bacteria were slightly lower than those of Gram-positive bacteria, which is consistent with the previous report.[27] The most significant antibacterial activity was observed with an MIC value of 16 μg/mL against three strains (*Pseudomonas aeruginosa, Escherichia coli* and *Salmonella typhimurium*). Herein, the antibacterial activity was increased up to approximately 8-fold compared with sialyllactose alone. In the case of *Salmonella typhimurium*, 2,6-sialyllactose-reduced AgNPs exhibited a lower MIC value (16 μg/mL) than that of 2,3-sialyllactose-reduced AgNPs (32 μg/mL).

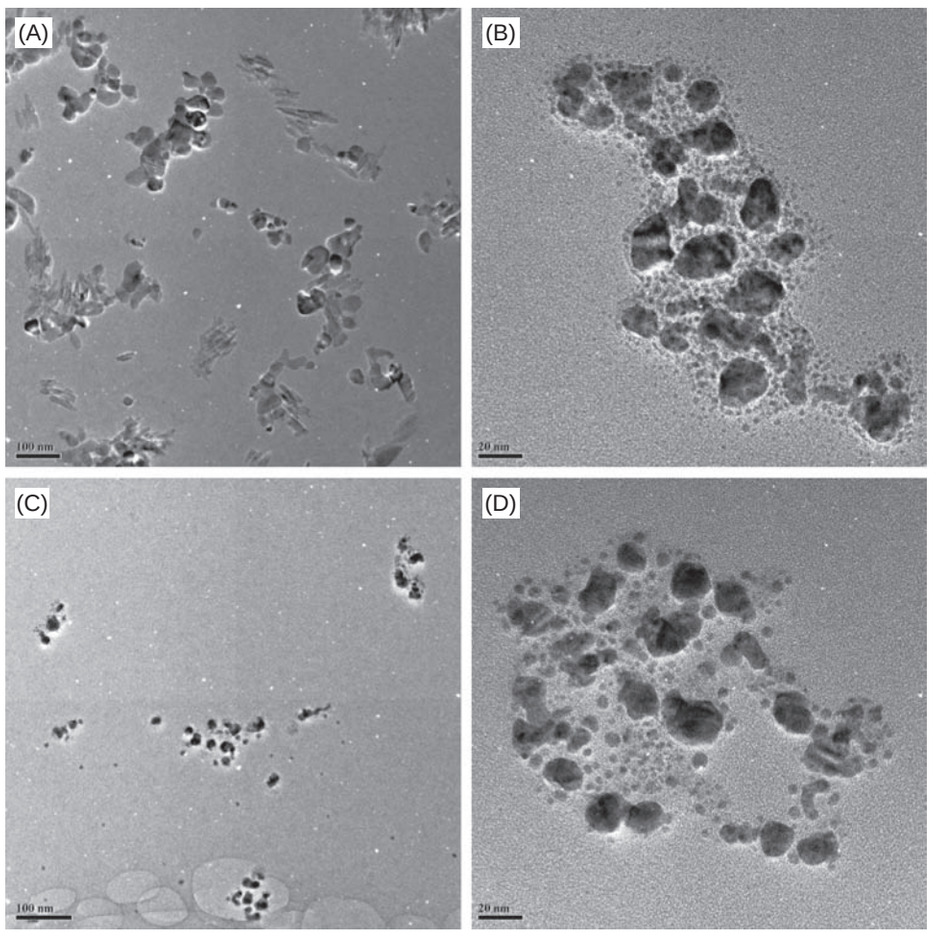

Fig. 9. HR-TEM images of 2,3-sialyllactose-reduced AgNPs before and after freeze-drying. Sucrose (50 mM) was added as a stabilizer. Sucrose was added after incubation in the oven. (A) and (B): before freeze-drying, (C) and (D): after freeze-drying. The scale bar represents (A) 100 nm, (B) 20 nm, (C) 100 nm, and (D) 20 nm.

RESEARCH ARTICLE

3.3. Effects of Stabilizers on the Freeze-Drying Process

For the application of AgNPs in pharmaceutical and biomedical arenas, an acceptable shelf life during shipping and storage is required. In general, the stabilization of biopharmaceutical formulations is conducted by drying in the presence of carbohydrate stabilizers. We adapted a freeze-drying process to lyophilize 2,3-sialyllactose-reduced AgNPs. When we reconstituted AgNPs after freeze-drying in the absence of a stabilizer, the AgNPs solution became colorless with black precipitates due to aggregation. The AgNPs solution also lost its characteristic SPR band. Thus, we tested four carbohydrates as stabilizers to increase the stability of AgNPs during a freeze-drying process: mannitol, sucrose, trehalose, and dextran. Mannitol, trehalose and sucrose do not have hemiacetal reducing ends while dextran possesses a reducing end. When adding mannitol (50–250 mM), the AgNPs solution tended to aggregate; therefore, we excluded mannitol in the following experiment. When sucrose, trehalose, and dextran were added during the mixing step on the hot plate (the preincubation step), complicated UV-Vis spectra were obtained with diverse colors of solution (yellow-orange-purple) (data not shown). This may be because the stabilizer itself also plays a role as a reducing agent. When a stabilizer was added after the formation of AgNPs by oven incubation, sucrose (50–250 mM) and trehalose (50–250 mM) exhibited excellent stability based on UV-Vis spectra (Figs. 8(A and B)). The color of the solution stayed yellow before and after freeze-drying in the presence of sucrose and trehalose for the entire range of concentrations tested (data not shown). When sucrose and trehalose were absent, the UV-Vis absorbance was significantly decreased after freeze-drying. As shown in Figure 8(C), dextran showed an increased peak width with increasing dextran concentration, which has a different UV-Vis profile compared to sucrose and trehalose. This may be because dextran possesses many hydroxyl functionalities as well as a reducing end, which may be involved in the reducing step of Ag ions to AgNPs. Therefore, the lowest concentration (50 mM) of sucrose and

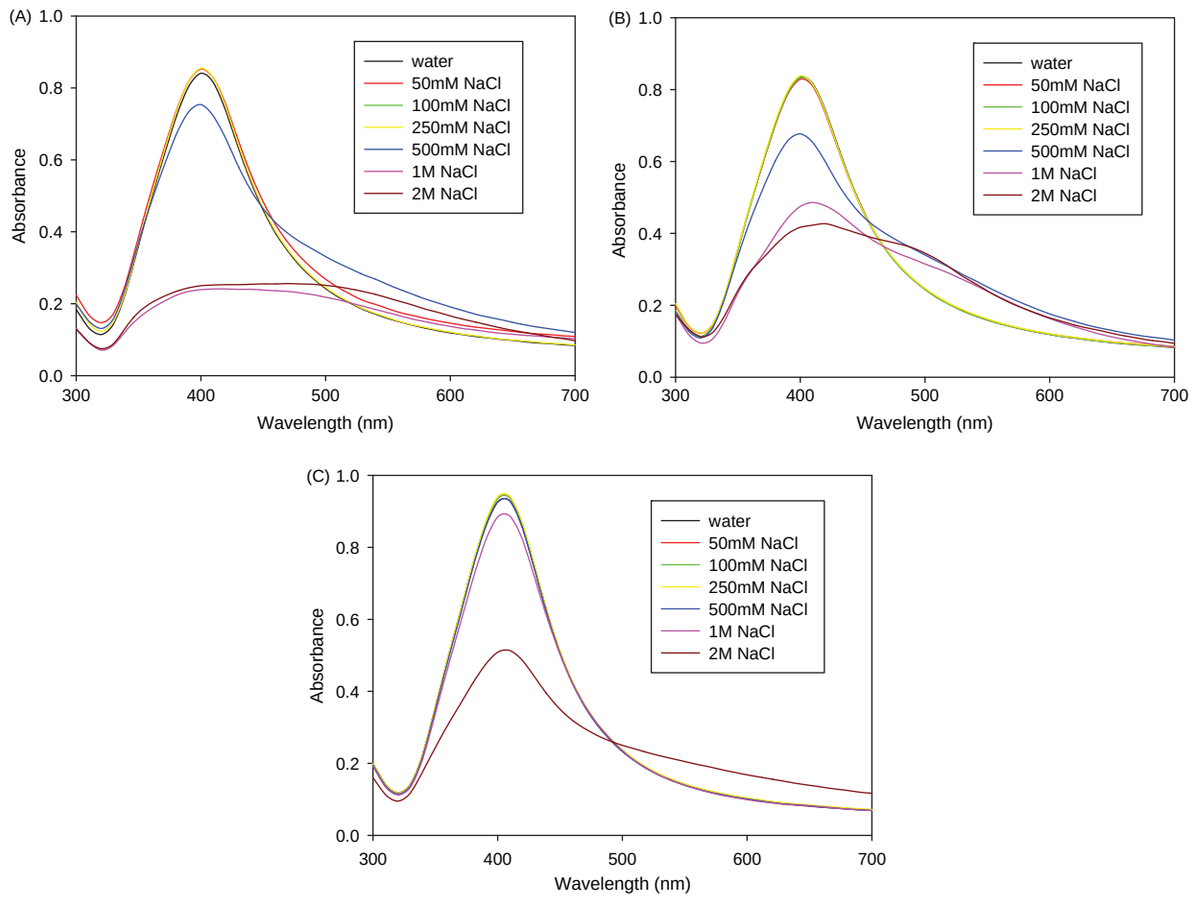

Fig. 10. Salt stability test. 2,3-Sialyllactose-reduced AgNPs were prepared under the optimum reaction conditions by oven incubation. (A) no stabilizer was added, (B) 50 mM sucrose was added as a stabilizer and no freeze-drying process was performed, (C) 50 mM sucrose was added as a stabilizer and a freeze-drying process was performed. The lyophilized powder was then reconstituted with double-distilled water to the original volume and UV-Vis spectra were recorded.

RESEARCH ARTICLE

trehalose was selected as an effective stabilizer to perform further experiments. As shown in the HR-TEM images of Figure 9, the freeze-drying process with the addition of stabilizers did not affect the shape and size of AgNPs considerably.

3.4. Salt and On-the-Shelf Stabilities

Next, we tested the salt stability of 2,3-sialyllactose-reduced AgNPs in the absence or presence of stabilizers (50 mM sucrose or trehalose). As shown in Figure 10(A), with the absence of stabilizers, the high salt addition (1 and 2 M NaCl) unstabilized AgNPs causing a loss of the characteristic SPR band. We observed a change of color from dark yellow to light yellow upon the initial addition of high salt. With further incubation at room temperature, the aggregation was observed with the high salt addition (1 and 2 M NaCl) where the color of the solution changed to colorless with black precipitates. The presence of 50 mM sucrose slightly improved the AgNPs solution stability (Fig. 10(B)), however, the SPR band was decreased with increasing NaCl concentration. Most interestingly, we observed that the freeze-drying process improved the salt stability of the AgNPs solution (Fig. 10(C)). Similar results were obtained when 50 mM trehalose was used as a stabilizer (data not shown). Sucrose and trehalose are commonly used for protein or nanosuspension drugs for stabilization during freeze-drying and storage.[28–33] It is known that the control of stabilization is accomplished by "glass dynamics" or by the specific interaction between biopharmaceuticals and carbohydrates that preserve native structure.[31] Although the mechanisms of sucrose and trehalose during the freeze-drying process in the AgNPs solution is not known, these stabilizers improved the salt stability of the AgNPs solution after freeze-drying. Further study is necessary to confirm this result. Excellent on-the-shelf stability was obtained before and after the freeze-drying process in the presence of 50 mM sucrose or 50 mM trehalose during 3 weeks, with the UV-Vis absorbance profile being maintained (data not shown). Currently, we test the on-the-shelf stability with a longer storage time.

4. CONCLUSION

In the present research, sialyllactose-reduced AgNPs were created with a green-synthetic approach and were successfully developed. The synthesis of AgNPs was confirmed by the SPR band, HR-TEM and AFM images, FT-IR spectra and DTA/TGA data. The stability of AgNPs was increased based on the SPR band by adding a stabilizer, with the efficient stabilizers determined to be sucrose and trehalose. Stabilizers provided excellent stability during the freeze-drying process as well as with the addition of salts and during storage on the shelf. Sialyllactose-reduced AgNPs exhibited an enhancement (approximately 8-fold) of antibacterial activities against *Pseudomonas aeruginosa, Escherichia coli* and *Salmonella typhimurium* when compared with sialyllactose alone. Sialyllactose-carrying molecules are known to inhibit influenza viruses by protecting the host cell from virus attachment on the cell surface. Therefore, sialyllactose-reduced AgNPs could exert synergistic effects by combining both the antibacterial activities of AgNPs and the antiviral activities of AgNPs and sialyllactose. Currently, the antiviral activity of AgNPs is being evaluated. These newly prepared Ag nanomaterials may have potential applications in the biomedical and pharmaceutical arenas in the treatment of both bacteria and influenza infections. In addition, the newly prepared Ag nanomaterials could be incorporated into diverse medical devices such as implants, catheters, bone cement, wound dressings, creams, surgical masks and bandages.

Acknowledgments: This work was supported by the Basic Science Research Program through the National Research Foundation of Korea (NRF) funded by the Ministry of Education, Science and Technology (2010-0004730 and 2010-18282). The financial support is gratefully acknowledged.

References and Notes

1. V. Edwards-Jones, *Lett. Appl. Microbiol.* 49, 147 **(2009)**.
2. M. Rai, A. Yadav, and A. Gade, *Biotechnol. Adv.* 27, 76 **(2009)**.
3. D. R. Monteiro, L. F. Gorup, A. S. Takamiya, A. C. Ruvollo-Filho, E. R. de Camargo, and D. B. Barbosa, *Int. J. Antimicrob. Agents* 34, 103 **(2009)**.
4. H. H. Lara, E. N. Garza-Treviño, L. Ixtepan-Turrent, and D. K. Singh, *J. Nanobiotechnol.* 9, 30 **(2011)**.
5. A. Nanda and M. Saravanan, *Nanomedicine-UK* 5, 452 **(2009)**.
6. A. M. Fayaz, K. Balaji, M. Girilal, R. Yadav, P. T. Kalaichelvan, and R. Venketesan, *Nanomed-Nanotechnol.* 6, 103 **(2009)**.
7. R. Bhattacharya and P. Mukherjee, *Adv. Drug Deliver. Rev.* 60, 1289 **(2008)**.
8. J. Tain, K. K. Y. Wong, C. M. Ho, C. N. Lok, W. Y. Yu, C. M. Che, J. F. Chiu, and P. K. Tam, *ChemMedChem* 2, 129 **(2007)**.
9. S. Galdiero, A. Falanga, M. Vitiello, M. Cantisani, V. Marra, and M. Galdiero, *Molecules* 16, 8894 **(2011)**.
10. V. K. Sharma, R. A. Yngard, and Y. Lin, *Adv. Colloid Interfac.* 145, 83 **(2009)**.
11. K. B. Narayanan and N. Sakthivel, *Adv. Colloid Interfac.* 169, 59 **(2011)**.
12. D. Wei, W. Sun, W. Qian, Y. Ye, and X. Ma, *Carbohyd. Res.* 344, 2375 **(2009)**.
13. X. Chen and A. Varki, *ACS Chem. Biol.* 5, 163 **(2010)**.
14. H. Oka, T. Onaga, T. Koyama, C. T. Guo, Y. Suzuki, Y. Esumi, K. Hatano, D. Terunuma, and K. Matsuoka, *Med. Chem. Lett.* 18, 4405 **(2008)**.
15. H. Oka, T. Onaga, T. Koyama, C. T. Guo, Y. Suzuki, Y. Esumi, K. Hatano, D. Terunuma, and K. Matsuoka, *Bioorg. Med. Chem. Lett.* 17, 5465 **(2009)**.
16. A. Tsuchida, K. Kobayashi, N. Matsubara, T. Muramatsu, T. Suzuki, and Y. Suzuki, *Glycoconjugate J.* 15, 1047 **(1998)**.
17. F. Feng, N. Miura, N. Isoda, Y. Sakoda, M. Okamatsu, H. Kida, and S. Nishimura, *Bioorg. Med. Chem. Lett.* 20, 3772 **(2010)**.

RESEARCH ARTICLE

18. S. M. Johansson, N. Arnberg, M. Elofsson, G. Wadell, and J. Kihlberg, *ChemBioChem* 6, 358 **(2005)**.
19. I. Papp, C. Sieben, K. Ludwig, M. Poskamp, C. Böttcher, S. Schlecht, R. Herrmann, and R. Haag, *Small* 6, 2900 **(2010)**.
20. M. M. Kemp, A. Kumar, S. Mousa, E. Dyskin, M. Yalcin, P. Ajayan, R. J. Linhardt, and S. A. Mousa, *Nanotechnology* 20, 455104 **(2009)**.
21. Clinical and Laboratory Standards Institute. M100-S17, P. Wayne: CLSI **(2007)**.
22. D. Wei and W Qian, *Colloid. Surface. B* 62, 136 **(2008)**.
23. L. Jin and R. Bai, *Langmuir* 18, 9765 **(2002)**.
24. M. Guzman, J. Dille, and S. Godet, *Nanomed-Nanotechnol.* 8, 37 **(2012)**.
25. J. R. Morones, J. L. Elechiguerra, A. Camacho, K. Holt, J. B. Kouri, J. T. Ramirez, and M. J. Yacaman, *Nanotechnology* 16, 2346 **(2005)**.
26. G. A. Sotiriou and S. E. Pratsinis, *Environ. Sci. Technol.* 44, 5649 **(2010)**.
27. S. Shrivastava, T. Bera, A. Roy, G. Singh, P. Ramachandrarao, and D. Dash, *Nanotechnology* 18, 225103 **(2007)**.
28. N. Perez-Moral, C. Adent, T. R. Noel, and R. Parker, *Eur. J. Pharm. Biopharm.* 78, 264 **(2011)**.
29. S. Kamiya, T. Kurita, A. Miyagishima, and M. Arakawa, *Drug Dev. Ind. Pharm.* 35, 1022 **(2009)**.
30. S. Toshioka, T. Miyazaki, Y. Aso, and T. Kawanishi, *Pharm. Res.* 24, 1660 **(2007)**.
31. L. Chang, D. Shepherd, J. Sun, D. Ouellette, K. L. Grant, X. Tang, and M. J. Pikal, *J. Pharm. Sci.* 94, 1427 **(2005)**.
32. P. O. Souillac, C. R. Middaugh, and J. H. Rytting, *Int. J. Pharm.* 235, 207 **(2002)**.
33. M. Holzer, V. Vogel, W. Mäntele, D. Schwartz, W. Hasse, and K. Langer, *Eur. J. Pharm. Biopharm.* 72, 428 **(2009)**.

Received: 26 December 2011. Accepted: 11 February 2012.

RESEARCH ARTICLE